Module 4: Interferometry

Lecture 20: Extraction of temperature data

The Lecture Contains:

- Data Reduction
  - Interferometry
  - Evaluation of Interferograms
  - Temperature Data Over a Grid

Previous Next

DATA REDUCTION

Principles of interferometry and the evaluation of interferograms for the determination of fringe temperature are discussed in the present section. It is shown that fringe in the infinite fringe setting are isotherms when the flow field is two-dimensional. More generally, fringes are isocontours of a path integral function of temperature.

Interferometry

In the infinite fringe setting, the optical path difference between the test and reference beam is zero in the absence of any thermal disturbance. Hence interference is constructive and a bright field-of-view is obtained. The image obtained is practically fringe-free, but may show imperfection associated with the spatial filter and the interferometer optics in the form of a single broad fringe. When non-isothermal condition prevail in the path of the test beam (i.e.,a candle flame) each ray of light undergoes a change of phase, depending on the extent of change of the refractive index of medium. Hence an optical path difference is established between the test and the reference beams, resulting in a fringe pattern. In the wedge fringe setting, the optical components are deliberately misaligned to produce a set of line fringes of any convenient spacing. In the presence of a thermal disturbance the fringes would be displaced towards regions of higher temperatures, thus producing a fringe pattern that resembles the temperature profile itself.

In the present discussion, attention is restricted to image patterns that from in the infinite fringe setting. Here, the test beam records information about the variation of the refractive index of the fluid. To make temperature measurement possible, the refractive index variation must be related to temperature. The relationship between the refractive index n and temperature T is established as follows. For transparent media, the Lorenz-Lorentz relationship holds.

$$\frac{n^2 - 1}{\rho(n^2 + 2)} = \text{constant} \tag{4}$$

For gases, the refractive index is closed to unity and the expression reduces to the Gladstone-Dale equation

$$\frac{n - 1}{\rho} = \text{constant} \tag{5}$$

where ρ is density. Hence $dn/d\rho = \text{constant}$. For moderate changes in temperature, typically $\leq 20\ K$ and nearly uniform bulk pressure, density varies linearly with temperature as

$$\rho = \rho_0(1 - \beta(T - T_0)) \tag{6}$$

it follow that dn/dT is also a constant, being purely a material property. Hence changes in temperature simultaneously result in changes in refractive index and from principles of wave optics, lead to changes in the phase of the wave. This is the origin of fringe formation in interformetric images.

more...

Evaluation of Interferograms

The thinned fringes essentially carry the information of the path integrated temperature field. Hence to extract temperature profiles and heat transfer rates from the interferogram, it is fringe skeleton rather that the fringe band that is needed. In the context of three-dimensional reconstruction of the temperature field, the line integral of the temperature field is required over a uniform grid so that topographic algorithms can be applied. Consequently the calculation of methodology adopted for the calculation of fringe temperature associated with the fringes is an important step in interferometry. The technique has been discussed in the context of an experiment with a differentially in this section. The technique has been discussed in the context of an experiment with a differentially with a differentially heated fluid layer.

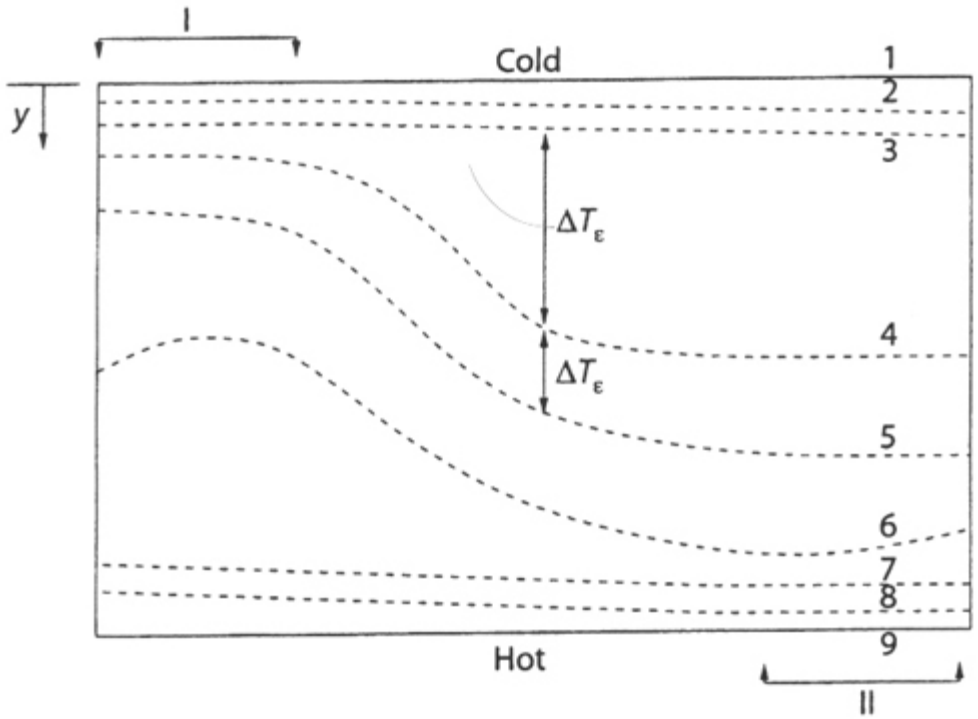

Figure 4.31: Calculation of the fringe temperature from an idealized fringe skeleton

For definiteness, consider the fringe skeleton as shown in figure 4.31. The upper and lower walls as shown in the figure have known temperatures. It is possible that high temperature gradients near the wall produce a large number of thin fringes. Hence during the recording and processing of the interferogram a few near wall fringes could be lost. The loss of near wall fringes could be due to the finite resolution the CCD camera, and loss of signal information during filtering and other image processing operations. The first fringe seen in a thinned interferogram near the wall will thus be of arbitrary order. One cannot assign a temperature to the fringes directly from the wall temperature though the wall itself is an is an isotherm. Even when no near-wall fringe is lost, assigning a temperature to the first fringe is not straight-forward since the wall (though an isotherm) need not be a fringe i.e., a site for destructive interference. The following procedure has been adopted in the present work to derive temperature values at the fringes.

Previous Next

Over the interferograms, two regions were selected, one where the fringes are close to the cold wall (marked I in fig.4.31) and the other where the fringes are close to the hot wall (marked II in fig 4.31). Two sets of independent calculations were performed to obtain all the fringe temperatures in the interferogram. The estimates of fringe temperature from both regions were found to be within 1%.. The fringe temperatures then allotted was the average of the estimates. Consider the fringes marked 2, 3, 4 (region I, cold wall) in figure 4.31. Fitting a function of the type

$$T(y) = a + by + cy^2$$

where y is a vertical coordinate, one obtains

$$\Delta T_\varepsilon = T_2 - T_3 = b(y_2 - y_3) + c(y_2^2 - y_3^2)$$

$$\Delta T_\varepsilon = T_3 T_4 = b(y_3 - y_4) + c(y_3^2 - y_4^2)$$

These two equations can be solved for the constants $b\ and\ c$. Here ΔT_ε, is the temperature change per fringe shift and y is a local coordinate measured from the upper wall.

The local wall temperature gradient is simply $(\partial T/\partial y)_{y=y1}$. From Equation (15), this gradient can be expressed as $(b + 2cy_1)$. The gradient in the temperature field very near the wall is likely to be constant since conduction heat transfer is dominant. Hence the gradient in temperature field at the first (fringe marked 2 in fig. 4.31) is expected to be same as the first gradient at the wall in region I. The gradient in temperature field at the first fringe is $(b + 2cy_2)$. The wall temperature gradient is allotted as an extrapolation step, the average of the two gradients. Once the gradient at the wall is known, the fringe temperature near the cold wall can be calculated as

$$T_2 = (y_2 - y_1)\frac{(b + 2cy_1) + (b + 2cy_2)}{0.5} + T_1$$

Since ΔT_ε, the temperature different between successive fringes is known, the subsequent fringe temperatures are found out by simply adding or subtracting the amount from the fringe temperature depending upon the sign of the temperature gradient. Since the image is a available in the form of a matrix, the above procedure for calculating the fringe temperature can be implanted at any column. The column where the near-wall fringes are dense (as in regions I and II) is preferred for this purpose. Column–to-column variation in the computed fringe temperatures was found to be generally small for the interferograms recorded in the experiments.

Previous Next

Temperature Data over a Grid

Once the absolute fringe temperatures are obtained, this data must be transferred to a two-dimensional uniform grid over the fluid region. This is required to apply tomographic algorithms for the reconstruction of the three-dimensional temperature field. The data transfer is achieved by interpolation as described below. The nine different points where the fringes intersect the column (fig. 4.32) are first mapped to a uniform rectangular grid using a quadratic polynomial as a basis. Temperature at any point (such as P, fig. 4.32) can be computed by using two-dimensional quadratic interpolation again. Interpolation using a higher order schemes can produce oscillations in the interpolated data. Consequently, the interpolated value in the interior may exceed the values at boundary points and is thus undesirable. Though rare, this may occur when the data spacing is large. In the present study, such overshoot and undershoot have been taken care of by using the idea of universal limiters. The limiter used is one-dimensional in the sense that it is applied only along the vertical direction. Once the interpolated value at a point on the superimposed grid is obtained, its value is compared with the two nearest vertically separated fringes. If the interpolated temperature is outside the range of the two fringe temperatures, the limiter is switched on to force the interpolated value to be one of the temperatures closest to the interpolated value. Interpolation errors in the present work were found to be negligible $(< 0.1\%)$.

The collection of thinned images from the Rayleigh-Benard experiment at a 90 degrees projection angle is shown in Figure 4.33. Interpolation has been carried over the entire image by superimposing a two-dimensional grid on it. The grid has 120 point along the horizontal and 21 points along the vertical direction. Once the interpolation is complete isotherms have been drawn to represent the fringes in the original image. This is shown in Figure 4.34. It can be seen here that the temperature data on the grid follows closely the pattern of the original thinned image and interpolation errors are negligible. The isotherms based on the interpolated grid data are seen to capture the lost fringes in the interferogram as well. Hence the isotherms in Figure 4.34 show all the fringes with continuity throughout the width of the cavity.

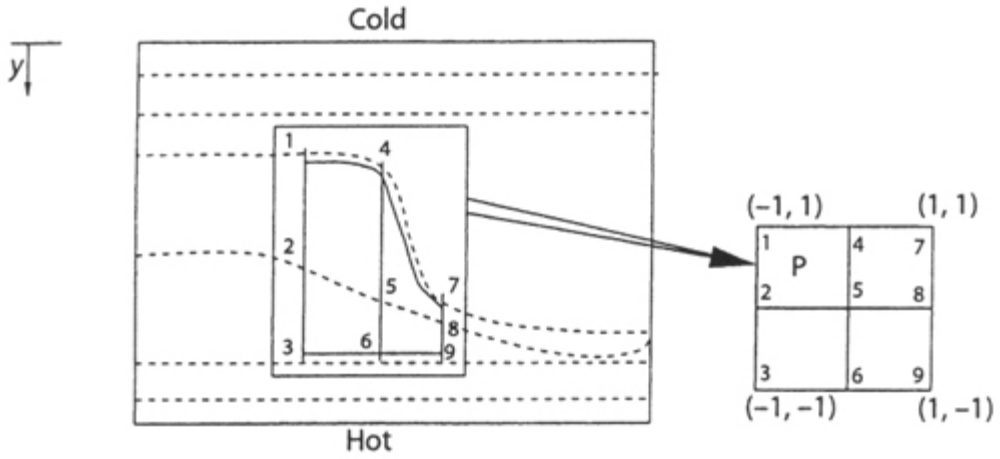

Figure 4.32: Data transfer from an interferogram to a two dimensional grid.

The correctness of fringe thinning, assigning fringe temperatures, and a check on the magnitude of interpolation errors have been examined by using the following result: At steady state, the width-average of the line integrals of temperature field plotted as a function of the vertical coordinate is independent of the projection angle. This is because the total energy transferred across the cavity is unchanged from one horizontal plane to the next. Figure 4.35 shown the variation of line integrals of the temperature field averaged over a horizontal plane as a function of the vertical coordinate. The line integrals are simply the temperature as conputed from the interferograms.

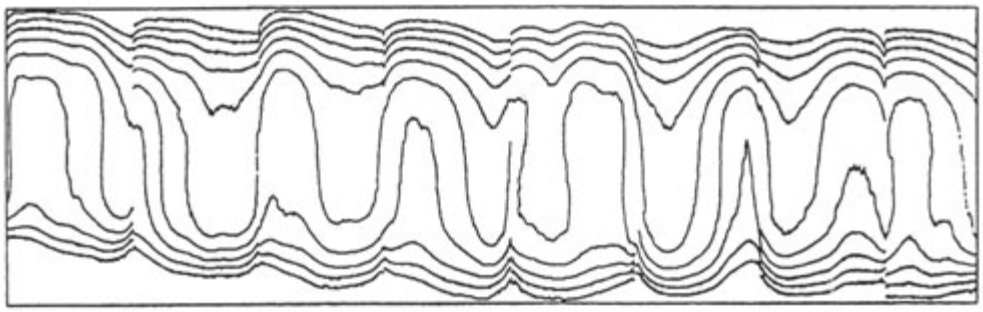

Figure 4.33: Collection of thinned images.

The y coordinate is measured from the cold top wall. Both zero and 90 degree projections have been shown and the Rayleigh number based on the temperature different across the across the fluid layer is 13900. The corresponding graph for $Ra = 40200$ is shown in Figure 4.36. The S-shaped curve, characteristic of buoyancy–driven convection can be seen in all the figures. The curve for the two projections match closely and their slopes at the hot and cold walls are practically equal. Temperature in the zero and 90 degree data have been subsequently corrected to ensure that between the two projections, the S-shaped curve is strictly unique. This step does not alter the isotherms in the projection data to any significant degree, but is expected to improve the convergence of the tomographic inversion process.

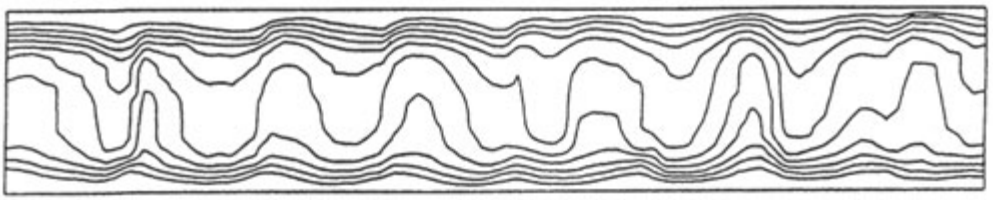

Figure 4.34: Isotherms obtained from the interpolated data

If temperature differences within the physical region being studied are large, two factors arise which limit the usefulness of interferometry. These are: (1) the linearity of relationship between density and temperature, and (2) beam deflection due to a refractive index gradient. These factors complicate the data reduction process and make interferometry more of a qualitative tool. However, fringes continue to form and images can be used for flow visualization tool. However, fringes continue to form and images can be used for flow visualization. In the present study, temperature differences between the test section and the ambient are within 20 K and the linear relation between the test section and the temperature has been taken to be valid.

Let $n(x,y)$ and $T(x,y)$ be the refractive index and temperature field respectively, the physical domain being a two-dimensional horizontal plane. A three–dimensional regional can be visualized as a collection of two-dimensional horizontal planes. Let n_0 and T_0 be the reference values of n and T respectively as encountered by the reference beam. Let L be the total geometric path length covered individually by the test and reference beams. The interferogram is a fringe pattern arising from the optical path difference

$$\Delta PL = \int_0^L (n(x,y) - n_0)ds \tag{7}$$

Difference between $n(x,y)$ and n_0 occur only over the length of the test cell. Hence L can be taken directly to be the length of the test cell. In terms of temperature, the difference in the path can be expressed as

$$\Delta PL = \frac{dn}{dT}\int_0^L (T(x,y) - T_0)ds \tag{8}$$

The integral is evaluated along the path of a light ray given by the coordinate s. Neglecting refraction effects, this path will be a straight line and the integral evaluation is greatly simplified. The fringes seen on the interferograms are a locus of points having the same optical path difference. Hence on any fringe the optical path difference ΔPL is a constant and

$$\int_0^L (T(x,y) - T_0)ds = \frac{\Delta PL}{dn/dT} = \text{constant}$$

Hence,

$$\int_0^L T(x,y)ds - T_0 L = \text{constant}$$

Previous Next

The integral $\int_0^L T(x,y)ds$ is defined as $\bar{T}L$, where $\bar{T}$ is the average value of $T(x,y)$ over the length L of the laser beam through the test cell. This is also the line integral of the function $T(x,y)$. Hence

$$L(\bar{T} - T_0) = \text{constant} \tag{9}$$

In the infinite fringe setting Equation (9) holds good for all fringes. When is constant for all the rays, Equation (9) implies that is a constant over the fringe and hence each fringe represents a locus of points over which the average of the temperature field along the direction of the ray is a constant; in this sense, fringes are isotherms.

Consider a geometry where the length of the ray through the test cell changes for each ray. The line integral of the function $T(x,y)(=\overline{T_2})$ at a location which corresponds to a length L_2 can be given in terms of the line integral of the function $T(x,y)(=\bar{T}_1)$ at some other location corresponding to a ray length of L_1 as

$$\overline{T_2} = T_0 + \frac{L_1}{L_2}(\bar{T}_1 - T_0) \tag{10}$$

Since the change in path length per fringe shift is a constant, the temperature drop per fringe shift is a also a constant. Defining the function $L(\bar{T} - T_0)$ in Equation (9) as $f(\bar{T}, L)$, the fringe temperature on two successive fringes for same value of L can be given as

$$\text{fringe 1} \quad f_1(\bar{T}, L) = \frac{\Delta PL}{dn/d\bar{T}}$$

$$\text{fringe2} \quad f_2(\bar{T}, L) = \frac{\lambda + \Delta PL}{dn/d\bar{T}}$$

where λ is the wavelength of the laser used. From these two equations, the temperature change per fringe shift can be calculated as

$$\Delta T_s = \frac{1}{L}\left(f_2(\bar{T},L) - f_1(\bar{T},L)\right) = \frac{\lambda/L}{dn/dT} \tag{11}$$

The interferogram reflects the equation

$$\Delta PL = \frac{dn}{dt}\int_0^L (T - T_0)ds$$

This shows that the fringe patterns contain information about the line integral of the temperature field. The set of all line integrals (an interferogram, in the present study) defines a projection of the temperature field. The interferograms can be numerically processed so that the left side of the above equation is a known quantity. The mathematical problem now is one of solving the temperature field from its projections. If the original field is three-dimensional, its projection is a field in a dimension reduced by unity, i.e., two for the present case. It is theoretically possible to record a large number of projections of the field at various angles and reconstruct the original temperature function with accuracy. This process of three-dimensional reconstruction from two-dimensional projections, called

tomography, is discussed in later sections.

Previous Next

The above derivation of temperature difference between successive fringes will be modified in the presence of a strong refracting field. In the present context, a strong refracting field will arise when a large transverse temperature gradient is present. The light ray will not travel in a single horizontal plane, and depending on the sign of the temperature gradient, the ray will bend in the vertical plane owing to refraction effects. Refraction, thus will introduce an additional optical path length to the test beam. Refraction effects can be precisely computer and accounted for. The extent of refraction determines the type of the three-dimensional reconstruction algorithm errors was found to be negligible and hence a sequence a sequential plane-by plane reconstruction approach was possible.

An estimate of the increase in path length due to refraction is developed here. Following Goldstein [4], consider the path of the light ray through a test cell (Figure: 4.30) when it is affected by the refraction effects. Let α be the bending angle at a location P of the test cell. The optical path length from A to B is given by:

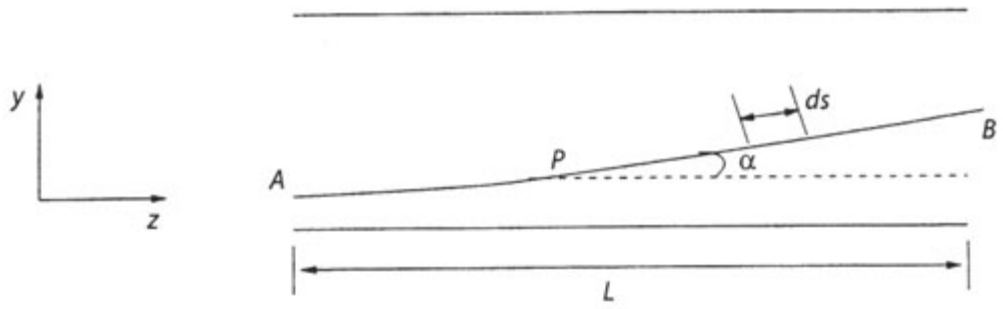

Figure 4.30: Calculation of bending angle of light ray due to refraction effects.

$$AB = \int_0^L n(x,y,z)ds = \int_0^L n(x,y,z)\frac{ds}{\cos\alpha}$$

Here y is a coordinate parallel to the gravity vector and z is parallel to the direction of propagation of light. Assuming α is small, $\cos\alpha$ can be expressed as

$$\cos\alpha = (1-\alpha^2)^{1/2}$$

and further using the first two terms of the binomial expansion

$$\cos\alpha \approx 1 - \frac{\alpha^2}{2}$$

Hence the optical path length is given by

$$AB = \int_0^L n(x,y,z)\left(1-\frac{\alpha^2}{2}\right)^{-1}dz = \int_0^L n(x,y,z)\left(1+\frac{\alpha^2}{2}\right)dz$$

The angle $\alpha(z)$ at any location z can be calculated as described in next slide.

Previous Next

Consider figure (4.31) where two wave fronts at times $\tau \; and \; \tau + \Delta\tau$ are shown. At time τ the ray at a position z. After a time interval of $\Delta\tau$, the light has moved a distance of Δz. Hence

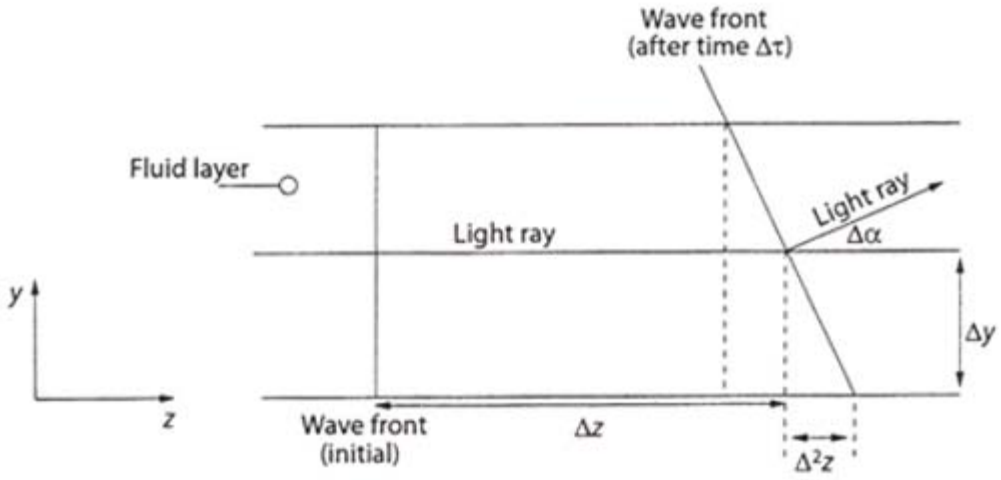

Figure 4.31 Bending of a light ray in a stratified fluid medium due to refraction

$$\Delta z = \Delta\tau \frac{C_0}{n}$$

where C_0 is the velocity of light in vacuum. There is a gradient in the refractive index along the y direction. The gradient in n results in a bending of the wave front due to refraction. The distance $\Delta^2 z$ is given by

$$\Delta^2 z = \Delta z_y - \Delta z_{y+\Delta y} \approx \Delta z_y - \Delta z_y + \frac{\Delta}{\Delta y}(\Delta z)\Delta y = C_0 \frac{\Delta 1/n(x,y,z)}{\Delta y}\Delta\tau\Delta y$$

Let $\Delta\alpha$ represents the bending angle at a fixed location. For a small increment in the angle, $\Delta\alpha$ can be expressed as

$$\Delta\alpha = \tan(\Delta\alpha) = \frac{\Delta^{2z}}{\Delta y} = -c_0 \frac{\Delta 1/n(x,y,z)}{\Delta y}\Delta\tau$$

$$= -n(x,y,z)\Delta z \frac{\Delta 1/n(x,y,z)}{\Delta y}$$

In the limiting case

$$d\alpha = \frac{1}{n(x,y,z)} \frac{\partial n(x,y,z)}{\partial y} dz \qquad (12)$$

Hence the cumulative blending angle at any location along the z axis is

$$\alpha(z) = \int_0^z \frac{1}{n(x,y,z)} \frac{\partial n(x,y,z)}{\partial y} dz$$

Previous Next

From Equation (12) the optical path length from A to B is

$$AB = \int_0^L n(x,y,z)\left(1+\frac{1}{2}\frac{1}{n^2}\left(\frac{\partial \bar{n}}{\partial y}\right)^{2z^2}\right)dz = \bar{n}(x,y,z)L + \frac{1}{6\bar{n}\ (x,y.z)}\left(\frac{\partial \bar{n}}{\partial y}\right)^2 L^3$$

where $\bar{n}(x,y,z)$ is the average line integral of $n(x,y,z)$ over the complete length L. Similarly the expressions $1/\overline{6n}$ and $\partial\bar{n}/\partial y$ represent average line integrals over the length L. The optical path length of the reference beam is simply

$$\text{Reference path} = \int_0^L n_0 dz = n_0 L$$

Hence the difference in the optical path length in the presence of refraction effects is the presence of refraction effects is

$$\Delta PL = \bar{n}(x,y,z)L + \frac{1}{\overline{6n}\ (x,y,z)}\left(\frac{\partial \bar{n}}{\partial y}\right)^2 L^3 - n_0 L$$

$$= (\bar{n}(x,y,z) - n_0)L + \frac{1}{\overline{6n}(x,y,z)}\left(\frac{\partial \bar{n}}{\partial y}\right)^2 L^3$$

$$= (\bar{T}_1\ (x,y,z) - T_0)L\frac{dn}{dT} + \frac{1}{\overline{6n}(x,y,z)}\left(\frac{\partial \bar{n}}{\partial y}\right)^2 L^3$$

Where $\bar{T}_1(x,y,z)$ represents the average line integral of the temperature field along the direction of the ray at a given point on the fringe. The corresponding ray over the next fringe traverses an additional distance of λ. Hence this can be written as

$$\Delta PL + \lambda = (\overline{T_2}(x,y,z) - T_0)L\frac{dn}{dT} + \frac{1}{\overline{6n}(x,y,z)}\left(\frac{\partial \bar{n}}{\partial y}\right)^2 L^3$$

where $\overline{T_2}(x,y,z)$ represents the average line integral of the temperature field along the direction of the ray at a given point on the fringe. The successive temperature field along the difference between two fringes can be computed from

$$\lambda = \left(\overline{T_2}(x,y,z) - \bar{T}_1(x,y,z)\right)L\frac{dn}{dT} + \frac{1}{\overline{6n}\ (x,y,z)}\left(\frac{dn}{dT}\right)^2 \times \left(\left(\frac{\partial T}{\partial y}\Big|_2\right)^2 - \left(\frac{\partial T}{\partial y}\Big|_1\right)^2\right)L^3 \quad (14)$$

and the temperature drop per fringe shift is

$$\Delta T_\varepsilon = \frac{1}{Ldn/dT}\left(\lambda - \frac{1}{\overline{6n}(x,y,z)}\left(\frac{dn}{dt}\right)^2\left(\left(\frac{\partial T}{\partial Y}\Big|_2\right)^2 - \left(\frac{\partial T}{\partial Y}\Big|_1\right)^2\right)L^3\right) \quad (15)$$

Previous Next

Since the gradient in the temperature field is known before the calculation of the fringe temperature the factor $\left(\frac{\partial T}{\partial y}\Big|_2\right) - \left(\frac{\partial T}{\partial y}\Big|_1\right)$ must be calculated from a guessed temperature field. Thus, the final calculation of ΔT_ε relies on a series of iterative steps with improved of the temperature gradients.

The refraction errors in the present set of experiments can be shown to be quite small. As a conservative estimate, the temperature gradient term can be replaced by its value at the wall. This would give an upper bound on the refraction error. For the following numerical values: $\lambda = 632.8\ nm, L = 0.5m, dn/dT$ for air at 20°C and [?] and refractive index of air at $20°C = 1.0$, the contribution of the refractive index term in Equation (14) can be evaluated as 2.617×10^{-8} This value is small as compared to the wavelength $(= 6328 \times 10^{-8} m)$

The number of fringes expected in a projection can be estimated directly from the relation

$$Number\ of\ fringes = \frac{T_{hot} - T_{cold}}{\Delta T_\varepsilon}$$

This equality was seen to be satisfied in all the experiments reported in the work. This also indicates that refraction errors in the present experiments are negligible.

Previous